SUPPLEMENTAL MATERIALS

Dual effects of the small-conductance Ca^{2+}-activated K^+ current on human atrial electrophysiology and Ca^{2+}-driven arrhythmogenesis: an *in silico* study

Nathaniel T. Herrera,[1] Xianwei Zhang,[1] Haibo Ni,[1] Mary M. Maleckar,[2] Jordi Heijman,[3] Dobromir Dobrev,[4,5,6] Eleonora Grandi,[1,@] Stefano Morotti[1,@]

[1] Department of Pharmacology, University of California Davis, Davis, CA, USA

[2] Computational Physiology Department, Simula Research Laboratory, Oslo, Norway

[3] Department of Cardiology, Cardiovascular Research Institute Maastricht, Faculty of Health, Medicine, and Life Sciences, Maastricht University, Maastricht, The Netherlands

[4] Institute of Pharmacology, West German Heart and Vascular Center, Faculty of Medicine, University Duisburg-Essen, Essen, Germany

[5] Department of Medicine, Montreal Heart Institute and Université de Montréal, Montréal, QC, Canada

[6] Department of Integrative Physiology, Baylor College of Medicine, Houston, TX, USA

[@] Correspondence to:

Stefano Morotti, PhD
Department of Pharmacology, University of California Davis, Davis, CA, USA
Email: smorotti@ucdavis.edu
Phone: 530-754-3341

Eleonora Grandi, PhD
Department of Pharmacology, University of California Davis, Davis, CA, USA
Email: ele.grandi@gmail.com
Phone: 530-752-4780

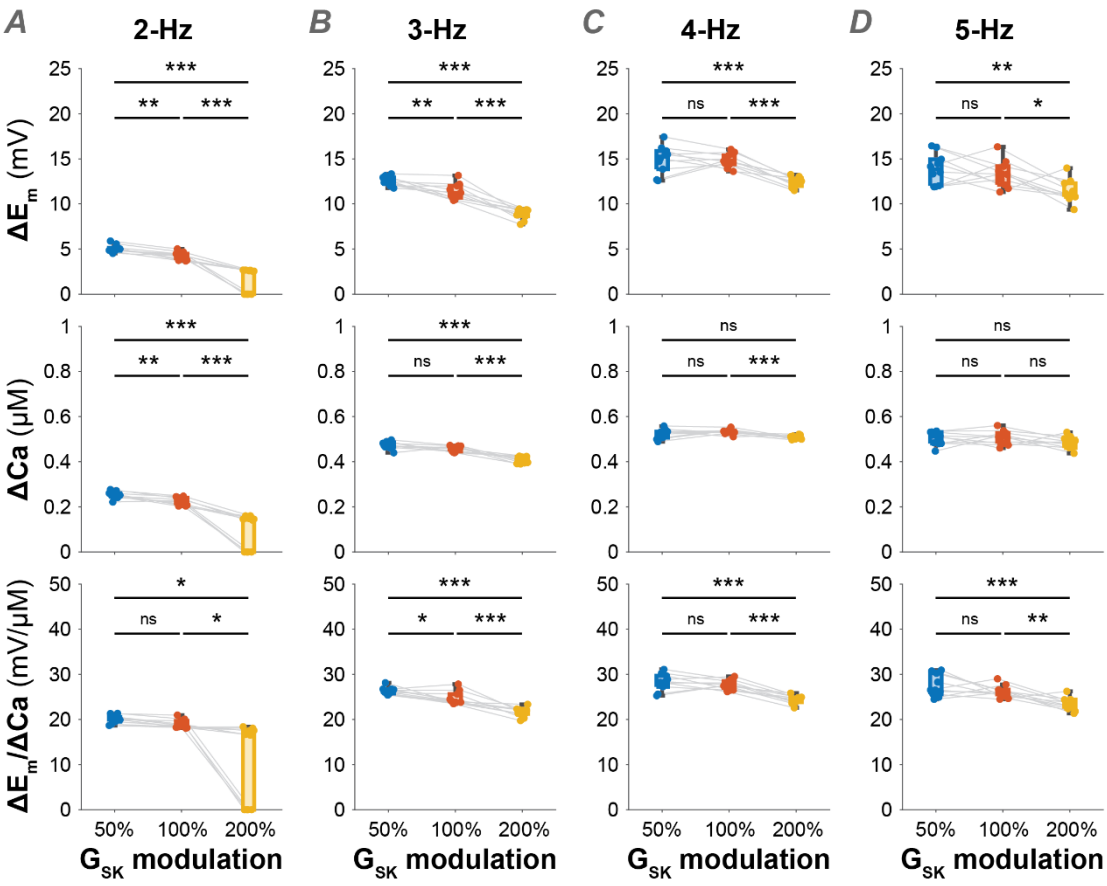

Figure S1. Increasing SK channel conductance enhances repolarization force over a broad range of pacing rates. The analysis shown in **Fig. 5B** and **C** was performed varying the stimulation frequency. No voltage or $[Ca^{2+}]_i$ oscillations were observed at 0.5 and 1-Hz pacing rates. We report here the summary data describing amplitude of membrane potential (E_m) and cytosolic Ca^{2+} concentration ($[Ca^{2+}]_i$) oscillations (ΔE_m and ΔCa), and the $\Delta E_m/\Delta Ca$ ratio in function of different values of SK channel maximal conductance (G_{SK}) at 2 (1), 3 (B), 4 (C), and 5 Hz (D). Null values of ΔE_m, ΔCa, and $\Delta E_m/\Delta Ca$ shown for 200% G_{SK} at 2-Hz pacing indicate absence of voltage or $[Ca^{2+}]_i$ oscillations. Statistical analysis was performed by one-way ANOVA with Bonferroni correction (***: $p < 0.001$; **: $p < 0.01$; *: $p < 0.05$; ns: not significant).

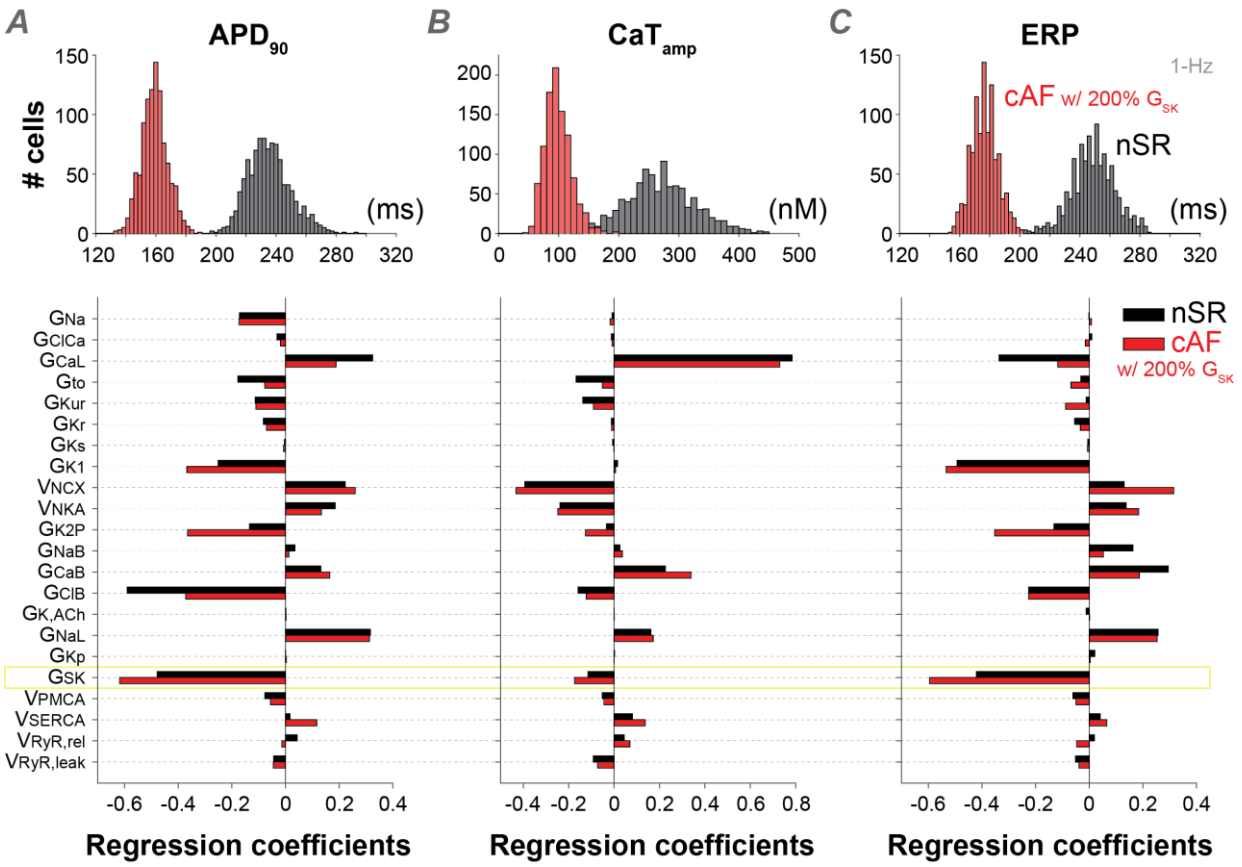

Figure S2. Sensitivity analysis performed simulating increased SK expression in chronic atrial fibrillation (cAF) vs. normal sinus rhythm (nSR). The analysis shown in **Fig. 2** was replicated assuming increased G_{SK} in cAF vs. nSR myocytes. Top panels report histograms showing the distribution of action potential duration (APD) at 90% repolarization (APD_{90}, A), Ca^{2+} transient amplitude (CaT_{amp}, B), and effective refractory period (ERP, C) assessed at 1-Hz pacing in nSR and cAF populations of 1,000 model variants. Bottom panels report the results of linear regression analysis performed to quantify the sensitivity of APD_{90}, CaT_{amp}, and ERP (assessed at 1-Hz pacing) to changes in the listed parameters in the nSR and cAF models. Simulated nSR data were obtained in a population of models built upon a baseline model with nominal SK channel maximal conductance (i.e., 100% G_{SK}). Simulated cAF data were obtained in a population of models built upon a baseline model with increased SK channel maximal conductance (i.e., 200% G_{SK}). Model variants exhibiting AP irregularities (1 in nSR, 4 in cAF) were excluded from the linear regression analysis.

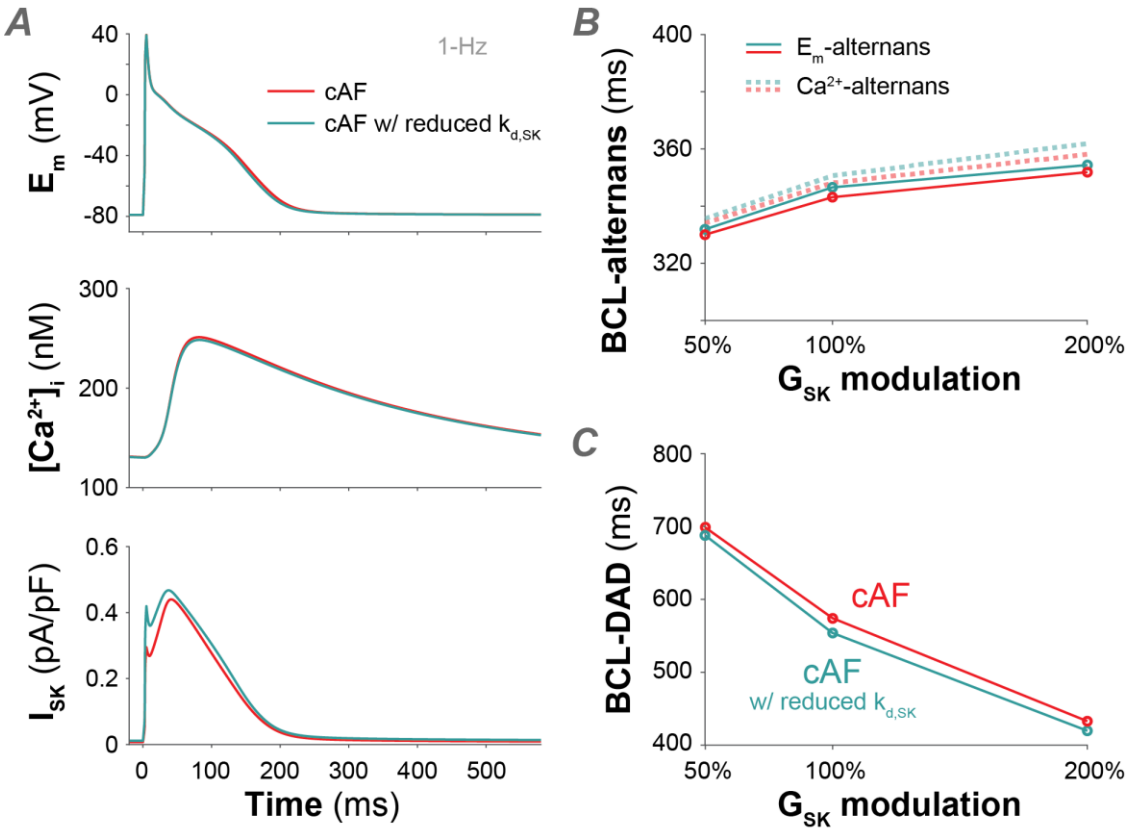

Figure S3. Increased SK channel Ca^{2+} affinity moderately affects atrial myocyte electrophysiology and arrhythmogenesis in cAF. A) Time course of E_m, $[Ca^{2+}]_i$, and SK current (I_{SK}) elicited in cAF myocytes during 1-Hz pacing with nominal (i.e., $K_{d,SK}$ = 350 nM) or increased (i.e., $K_{d,SK}$ = 230 nM) SK channel affinity for intracellular Ca^{2+}. B) Effect of $K_{d,SK}$ modulation on the maximal basic cycle length (BCL) required for inducing voltage (solid lines) and Ca^{2+} (dotted lines) alternans in the baseline cAF model. C) Effect of $K_{d,SK}$ modulation on the maximal BCL required for inducing delayed afterdepolarizations (DADs) in the baseline cAF model.

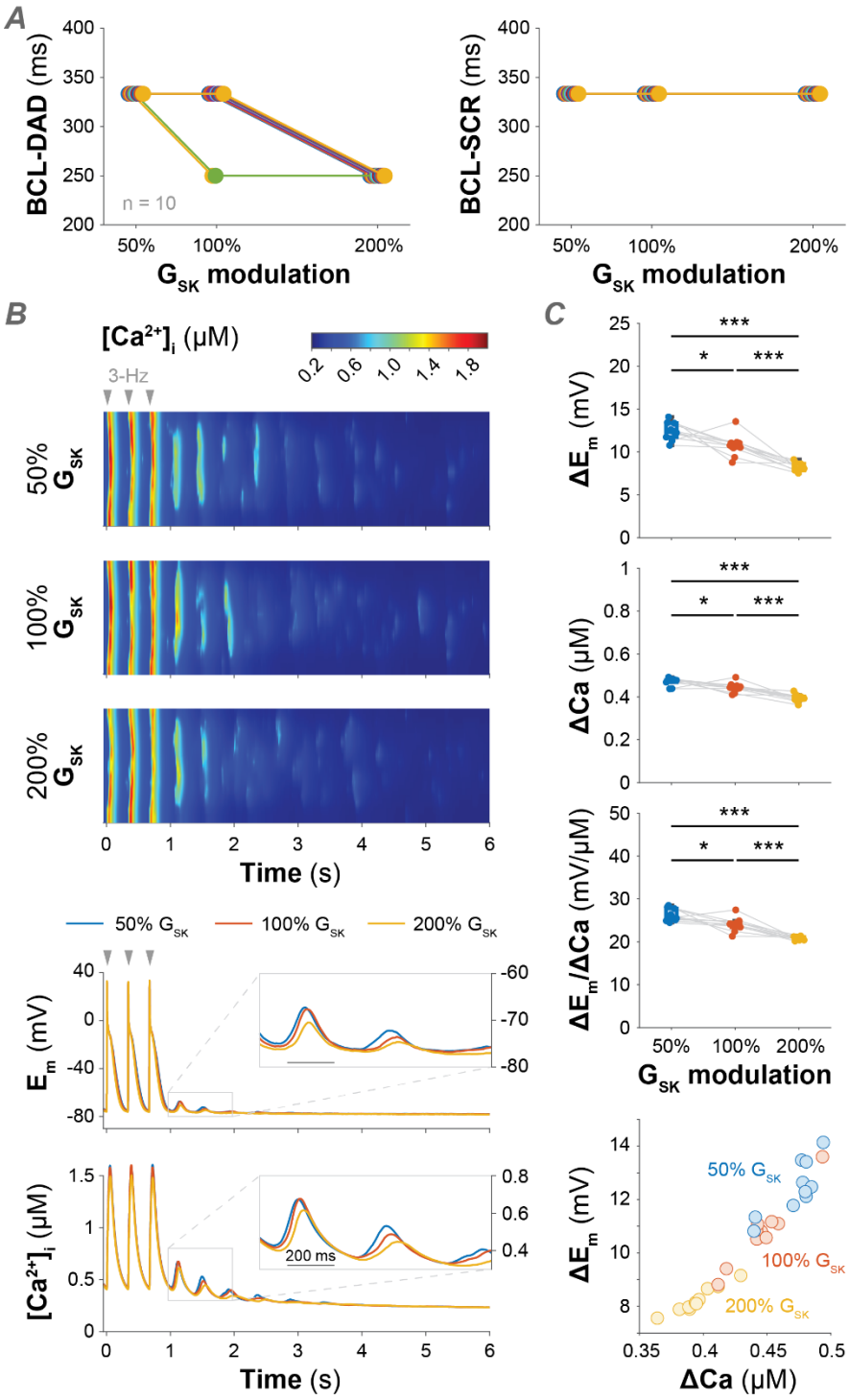

Figure S4. Increasing SK channel conductance enhances the repolarization force that counteracts DADs also when SK channel affinity for intracellular Ca^{2+} is increased. We replicated the simulations shown in **Fig. 5** with increased SK channel affinity for intracellular Ca^{2+} concentration (i.e., $K_{d,SK}$ reduced to 230 nM). A) Effect of changes in G_{SK} on the maximal basic cycle length (BCL) inducing delayed depolarizations (DADs) and spontaneous Ca^{2+} release events (SCRs) in the 3D atrial myocyte model. We used 10 mV and 300 nM as thresholds for

DADs and SCRs, respectively. The simulations were repeated for 10 randomly generated tubular structures with sparse tubular densities. B) Top panels show representative transverse line scans of local cytosolic Ca^{2+} concentration obtained pausing the electrical stimulation after a train of impulses at 3-Hz pacing for different G_{SK} values. The last three paced beats are reported in the figure. Bottom panels report the time course of corresponding global cytosolic Ca^{2+} concentration and membrane potential. C) Summary data resulting from simulating the protocol described in panel B in the 10 different tubular structures. Top panels show amplitude of E_m and $[Ca^{2+}]_i$ oscillations (ΔE_m and ΔCa), and the $\Delta E_m/\Delta Ca$ ratio in function of different G_{SK} values. Statistical analysis was performed by one-way ANOVA with Bonferroni correction (***: $p < 0.001$; **: $p < 0.01$; *: $p < 0.05$; ns: not significant). ΔE_m and ΔCa are also compared against each other in the scatter plot reported in the bottom panel.

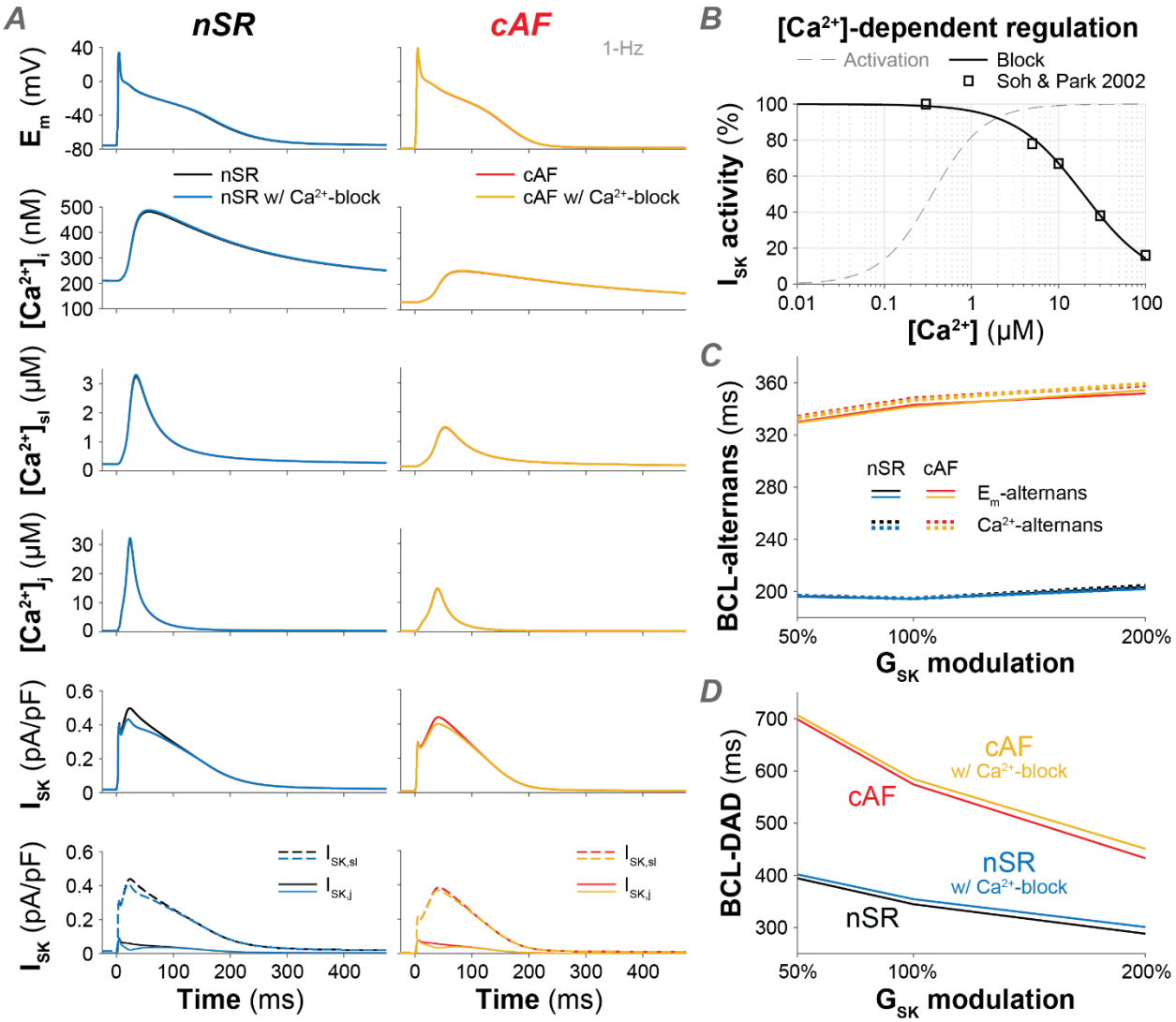

Figure S5. Inhibition of I_{SK} at high Ca^{2+} levels moderately affects atrial myocyte electrophysiology and arrhythmogenesis. A) Time course of E_m, Ca^{2+} transients in cytosolic, sub-sarcolemmal, and junctional cleft compartments ($[Ca^{2+}]_i$, $[Ca^{2+}]_{sl}$, and $[Ca^{2+}]_j$, respectively), and total SK current (I_{SK}) and its sub-sarcolemmal and junctional cleft components ($I_{SK,sl}$ and $I_{SK,j}$) elicited during 1-Hz pacing. These traces were obtained assuming that intracellular Ca^{2+} only causes I_{SK} activation (as done in all previous simulations), or that it also blocks I_{SK} at higher concentrations. B) Comparison between the formulations of Ca^{2+}-dependent I_{SK} activation ($K_{d,SK}$ = 350 nM, dashed line) and block (IC_{50} ≈ 20 μM, solid line) used in simulations. Ca^{2+}-dependent block is implemented as F_{block} = 1 - 1/(1+ exp((log$_{10}$(0.0193)-log$_{10}$([Ca^{2+}]))/0.4)), with [Ca^{2+}] expressed in mM. The symbols indicate the experimental data used to model Ca^{2+}-dependent block (Soh & Park, *Biophys J*. 2002 Nov;83(5):2528-38). C) Effect of Ca^{2+}-dependent block on the maximal BCL required for inducing voltage (solid lines) and Ca^{2+} (dotted lines) alternans in the baseline nSR and cAF models. D) Effect of Ca^{2+}-dependent block on the maximal BCL required for inducing DADs in the baseline nSR and cAF models.

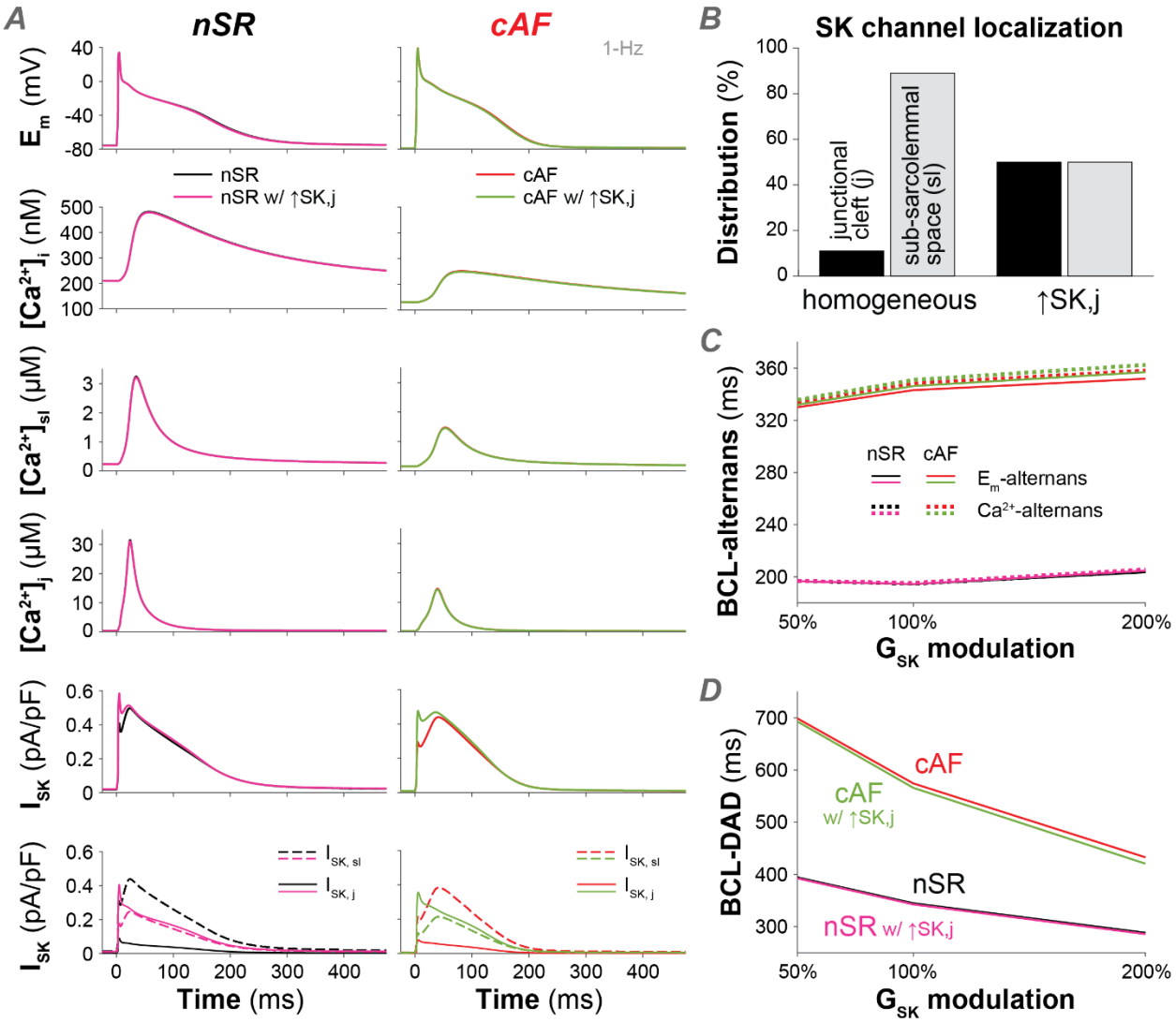

Figure S6. Increasing the density of SK channels in the junctional space minimally affects atrial myocyte electrophysiology and arrhythmogenesis. A) Time course of E_m, Ca^{2+} transients in cytosolic, sub-sarcolemmal, and junctional cleft compartments ($[Ca^{2+}]_i$, $[Ca^{2+}]_{sl}$, and $[Ca^{2+}]_j$, respectively), and total SK current (I_{SK}) and its sub-sarcolemmal and junctional cleft components ($I_{SK,sl}$ and $I_{SK,j}$) elicited during 1-Hz pacing. These traces were obtained assuming that homogeneous distribution of SK channels through the membrane (as done in all previous simulations), or increased SK channel density in the junctional space (↑SK,j). B) Bar graph showing the fractions of SK channels in sub-sarcolemmal (grey) and junctional cleft (black) compartments used in the two sets of simulations. Since the Grandi *et al*. framework was developed assuming that 89% of the membrane is non-junctional, 11% of SK channels are expressed the junctional space in case of homogeneous distribution. To simulate higher SK channel density in this compartment, this fraction was increased to 50%. C) Effect of increased density of SK channels in the junctional space on the maximal BCL required for inducing voltage (solid lines) and Ca^{2+} (dotted lines) alternans in the baseline nSR and cAF models. D) Effect of increased density of SK channels in the junctional space on the maximal BCL required for inducing DADs in the baseline nSR and cAF models.

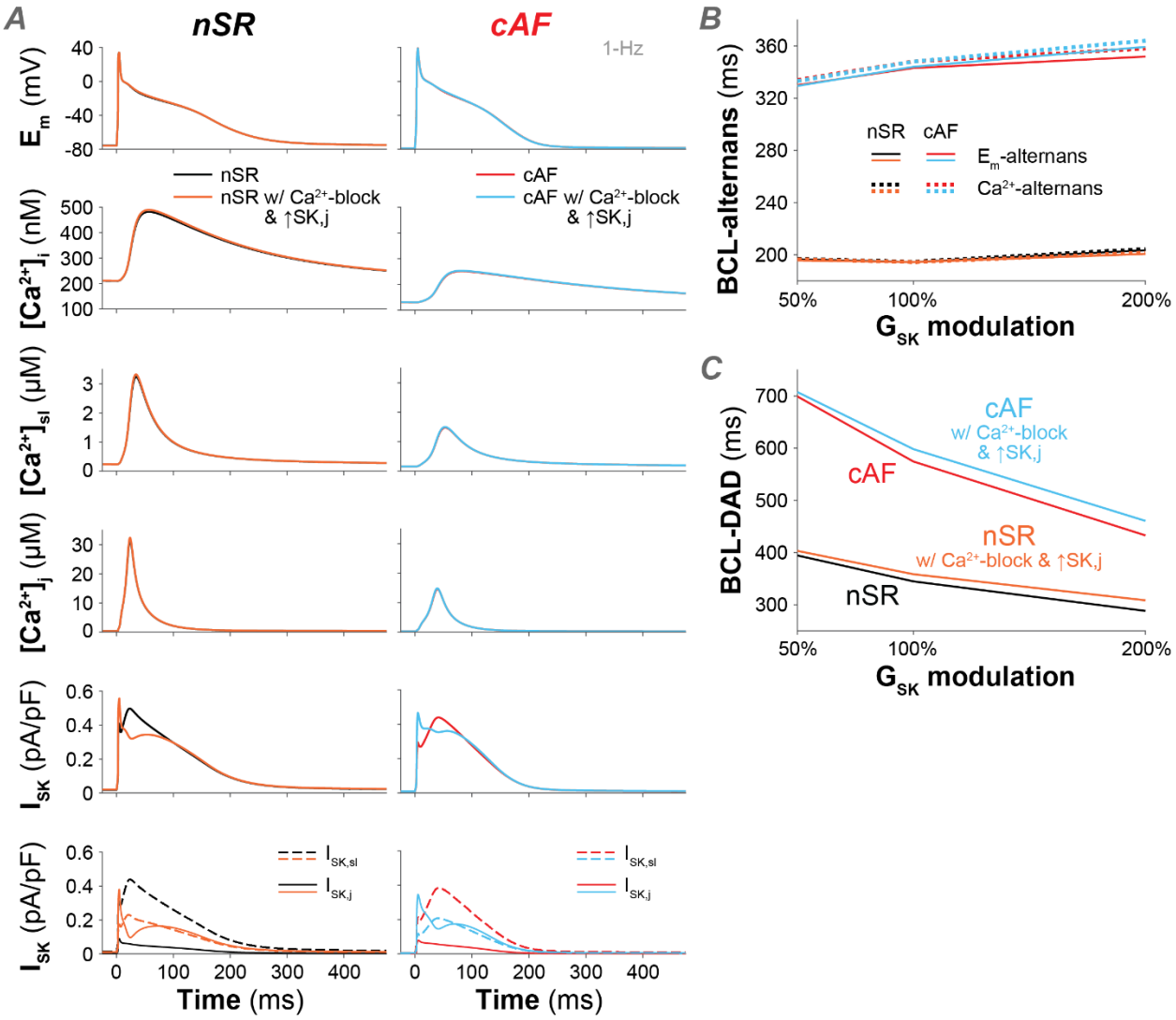

Figure S7. Increasing the density of SK channels in the junctional space enhances the effects of Ca^{2+}-dependent block of I_{SK}. A) Time course of E_m, Ca^{2+} transients in cytosolic, sub-sarcolemmal, and junctional cleft compartments ($[Ca^{2+}]_i$, $[Ca^{2+}]_{sl}$, and $[Ca^{2+}]_j$, respectively), and total SK current (I_{SK}) and its sub-sarcolemmal and junctional cleft components ($I_{SK,sl}$ and $I_{SK,j}$) elicited during 1-Hz pacing. These traces were obtained by simulating the following two conditions: *i)* intracellular Ca^{2+} only causes I_{SK} activation and SK channels are homogeneously distributed, and *ii)* combined inclusion of Ca^{2+}-dependent block (as described in **Fig. S5**) and increase in SK channels density in the junctional space (as described in **Fig. S6**). B) Effect of combined changes on the maximal BCL required for inducing voltage (solid lines) and Ca^{2+} (dotted lines) alternans in the baseline nSR and cAF models. C) Effect of combined changes on the maximal BCL required for inducing DADs in the baseline nSR and cAF models.